water

MDPI

Article

Adsorption Performance of Modified Fly Ash for Copper Ion Removal from Aqueous Solution

Gabriela Buema [1], Maria Harja [2,*], Nicoleta Lupu [1], Horia Chiriac [1], Loredana Forminte [2], Gabriela Ciobanu [2], Daniel Bucur [3,*] and Roxana Dana Bucur [3]

[1] National Institute of Research and Development for Technical Physics, 47 Mangeron Boulevard, 700050 Iasi, Romania; gbuema@phys-iasi.ro (G.B.); nicole@phys-iasi.ro (N.L.); hchiriac@phys-iasi.ro (H.C.)
[2] Faculty of Chemical Engineering and Environmental Protection, "Gheorghe Asachi" Technical University of Iasi, 73 Prof. dr. docent Dimitrie Mangeron Str., 700050 Iasi, Romania; loredanalitu@gmail.com (L.F.); gciobanu@tuiasi.ro (G.C.)
[3] Department of Pedotechnics, Faculty of Agriculture, University of Agricultural Sciences and Veterinary Medicine in Iasi, 3, Mihail Sadoveanu Alley, 700490 Iasi, Romania; rbucur@uaiasi.ro
* Correspondence: mharja@tuiasi.ro (M.H.); dbucur@uaiasi.ro (D.B.)

Abstract: The initial characteristics of Romanian fly ash from the CET II Holboca power plant show the feasibility of its application for the production of a new material with applicability in environmental decontamination. The material obtained was characterized using standard techniques: scanning electron microscopy (SEM), energy dispersive X-ray analysis (EDX), instrumental neutron activation analysis (INAA), X-ray diffraction (XRD), Fourier transform infrared spectroscopy (FTIR), the Brunauer–Emmett–Teller (BET) surface area, and thermogravimetric differential thermal analysis (TG-DTA). The adsorption capacity of the obtained material was evaluated in batch systems with different values of the initial Cu(II) ion concentration, pH, adsorbent dose, and contact time in order to optimize the adsorption process. According to the experimental data presented in this study, the adsorbent synthesized has a high adsorption capacity for copper ions (q_{max} = 27.32–58.48 mg/g). The alkali treatment of fly ash with NaOH improved the adsorption capacity of the obtained material compared to that of the untreated fly ash. Based on the kinetics results, the adsorption of copper ions onto synthesized material indicated the chemisorption mechanism. Notably, fly ash can be considered an important beginning in obtaining new materials with applicability to wastewater treatment.

Keywords: fly ash; copper ions; isotherms; kinetic models

Citation: Buema, G.; Harja, M.; Lupu, N.; Chiriac, H.; Forminte, L.; Ciobanu, G.; Bucur, D.; Bucur, R.D. Adsorption Performance of Modified Fly Ash for Copper Ion Removal from Aqueous Solution. *Water* **2021**, *13*, 207. https://doi.org/10.3390/w13020207

Received: 8 December 2020
Accepted: 13 January 2021
Published: 16 January 2021

1. Introduction

Fly ash is a manufactured product that comes from coal burning power plants. EU countries produce two million tons of fly ash every year, but only a fraction of it is capitalized on. Unfortunately, there is a serious issue associated with fly ash disposal because of its negative effects on air, water, and soil. This type of material contains principally SiO_2 and Al_2O_3 [1], elements that recommend the use of ash in a large spectrum of applications. For example, it is used for zeolite synthesis [2,3], as catalysts [4], in construction as filler or as a precursor for geopolymers [5–7], as an adsorbent [8–11], for ceramics [12,13], etc. Thus, many studies were involved in order to find a solution that would allow its utilization. Several studies have shown that one of the alternative applications is its use in heavy metal removal [14–16]. In particular, careful attention is required for the removal of Cu(II) from wastewater. Contamination with Cu(II) leads to liver and kidney diseases, insomnia, itching, and dermatitis [17–20]. Fly ash eliminates copper ions from wastewater, but the efficiency is low [21,22]. Cu(II) ions can be removed by many methods, such as chemical precipitation, ion exchange, membrane filtration, electrochemical treatments, coagulation/flocculation, and adsorption. However, the superiority of the adsorption technique is due to its simplicity, cost-effectiveness, and efficiency [23]. Although chemical

precipitation is one of the methods that is most often used to remove copper ions, it has the disadvantage that it requires a large amount of chemicals in order to reduce metals to an allowable level for discharge [24]. Compared to the chemical precipitation technique, adsorption can remove metals over a wider pH range and at lower concentrations [25]. It has been demonstrated by several studies that the chemical precipitation method is limited. Incomplete precipitation, the chemical instability of the precipitates, and the formation of large sludge volumes could occur [26].

Properties such as high treatment capacity, high removal efficiency, and fast kinetics recommend the ion-exchange processes to remove heavy metals from wastewater. On the other hand, they do have the disadvantage that ion exchange is highly sensitive to the pH of the solution. Membrane filtration is a pressure driven separation process for Cu(II) that is based on size exclusion and best performance. The electrochemical treatment needs a large capital investment in order to start the process and involves high maintenance costs. The coagulation–flocculation technique is used in the purification of water but must be followed by other treatment techniques [24].

The literature demonstrates that the adsorbents based on modified fly ash are more efficient in the adsorption process due to the higher specific surface area compared with fly ash ''as-cast" [21,23,27]. Based on the data published by Querol et al. [28], several researchers have studied the possibility of obtaining new materials based on fly ash by varying the working conditions. Depending on the experimental conditions and the chemical composition of the fly ash used, different materials are obtained. The principle of the method is based on the direct activation of the ash in a closed system with alkaline solutions (NaOH, KOH, LiOH).

One of the extensive applications of the treated fly ash is that it is used as a low-cost absorbent for the elimination of different heavy metal ions. The types of materials that could be obtained after the treatment of fly ash are related in Table 1.

Table 1. Types of materials synthesized from fly ash for Cu(II) removal.

Zeolite	Method of Synthesis	References
NaP1, Analcime and Chabazite	Hydrothermal method	[29]
4A	Hydrothermal method	[30]
Na–X, NaP, Na–S	Hydrothermal method	[31]
X	Fusion method	[32]

It has been demonstrated that the adsorption capacity of the modified fly ash largely depends on the method of activation [23,33–35].

In order to avoid the high cost of adsorbent, an easy and low-cost method was employed. Thus, this research is based on the idea of the application of the modified fly ash by direct activation at room temperature for 7 days as an adsorbent for copper ion adsorption.

The main objective of this research was the synthesis of fly ash with NaOH for its use in the adsorption of copper ions from aqueous solution.

The novelty of this study consists in the simple method of synthesis at room temperature, which does not involve high production costs. As far as we know, this type of method has not been proposed in the literature.

Firstly, the prepared adsorbent was characterized by various analytical techniques, such as scanning electron microscopy (SEM), energy dispersive X-ray analysis (EDX), instrumental neutron activation analysis (INAA), X-ray diffraction (XRD), Fourier transform infrared spectroscopy (FTIR), the Brunauer–Emmett–Teller (BET) surface area, and thermogravimetric differential thermal analysis (TG-DTA). The adsorption experiments were performed in batch mode in order to optimize some influential parameters: pH, adsorbent dose, initial concentration, and contact time. The experimental results were analyzed using three kinetic models: pseudo-first order, pseudo-second order, and intraparticle diffusion. At the end, the adsorption capacity of the material produced in this study was

compared with data obtained for other adsorbents involved in copper ion adsorption from aqueous solution.

2. Materials and Methods

2.1. Materials

The fly ash (FA) used in this work was from CET II (Iasi, Romania). According to the American Association for Testing and Materials (ASTM C618), the fly ash used in this study can be classified as class F. A detailed characterization was published previously. The raw fly ash used for the synthesis has a low adsorption capacity for copper ions, so some modification is necessary in order to improve the quality of this fly ash [36].

The chemical reagents involved in the treatment of fly ash (NaOH), respectively, in the adsorption measurements ($CuSO_4$ $5H_2O$, HCl, NaOH, rubeanic acid) from Sigma-Aldrich (St. Louis, MO, USA) were used.

Cu(II) initial concentrations of 300, 500, and 700 mg/L were prepared by dissolving predefined amounts of $CuSO4{\cdot}5H_2O$ in deionized water.

The basic characterization of the synthesized adsorbent (SEM, EDX, INAA, XRD, FTIR, BET surface area, and thermal analysis) was performed using the following equipment:

1. The morphology and the chemical composition were determined using a Vega Tescan 3 SBH (Brno, Czech Republic) and a QUANTA 3D-AL99/D8229 (FEI Company, Hillsboro, OR, USA);
2. The determination of the trace elements was performed using instrumental neutron activation analysis (INAA) at the 2 MW pool-type research reactor of the Technical University of Delph (Delph, The Netherlands) combined with high resolution c-ray spectroscopy.
3. The X-ray diffraction pattern was recorded using an X'PERT PRO MRD Diffractometer (PANalytical, Almelo, The Netherlands);
4. Fourier transform infrared spectroscopy (FTIR) was performed on a Thermo Scientific Nicolet 6700 FT-IR spectrometer;
5. Nitrogen physical sorption was carried out at –196 °C on an Autosorb 1-MP gas sorption system (Quantachrome Instruments, Boynton Beach, FL, USA);
6. The thermal analysis was performed with a METTLER TOLEDO TGA/SDTA 851;
7. The pH was measured with a pH-meter (Hanna Instruments, Cluj-Napoca, Romania), while a Spectrophotometer Buck Scientific was used for copper ion detection (Buck Scientific, East Norwalk, CT, USA).

2.2. Adsorbent Synthesis

FA was treated by 2 M NaOH solution. The mixture, with a 1/3 solid–liquid ratio, was intermittently stirred for 168 h at room temperature. Finally, the obtained material, denoted as MFA, was washed until it reached a neutral pH and dried in an oven at 60 °C for 24 h. The adsorbent obtained was considered to be MFA and it was stored.

2.3. Experimental Procedure

Batch adsorption experiments were performed in order to study the influence of different parameters through the adsorption capacity of Cu(II) ions by the MFA adsorbent. All of the tests were conducted at room temperature.

All of the results were carried out in triplicate.

The Cu(II) concentration in the supernatant was analyzed spectrophotometrically at 390 nm using rubeanic acid. In order to calculate the quantity of Cu(II) ions adsorbed per gram of adsorbent and the removal efficiency, R (%), the equations below were used:

$$q,\ mg/g = \frac{(C_0 - C_e)V}{m} \quad (1)$$

$$R,\ \% = \frac{(C_0 - C_e)}{C_0} x100 \quad (2)$$

where C_0 and C_e are the initial and equilibrium concentrations (mg/L), q is the amount of Cu adsorbed onto MFA (mg/g), V is the volume of the solution (L), and m is the quantity of MFA (g).

3. Results

3.1. Characterization of Adsorbent

This section investigated the characteristics of the MFA adsorbent. A comprehensive analysis from the SEM, EDX, INAA, XRD, FTIR, and BET surface area points of view is presented.

The surface properties of the adsorbent were examined through the SEM technique. Additionally, the SEM image of fly ash is represented in Figure 1 in order to provide a better visualization and to determine if the treatment with NaOH contributed to the modification of the surface of the fly ash material. The SEM image of the MFA adsorbent compared with unmodified fly ash is illustrated in Figure 1. In general, fly ash particles are predominantly spherical in shape with a relatively smooth surface texture. According to Figure 1, after NaOH treatment, a structure with crystals in the form of a few elongated rods is clearly displayed by the MFA material. It can be highlighted that the activation time of 168 h has a significant influence on the morphology.

An EDX mapping image was used to find the elements present in the MFA adsorbent.

The EDX evaluation related in Table 2 shows that oxygen (33.85 wt%), silica (18.89 wt%), and aluminum (18.33 wt%) are the basic elements of the MFA adsorbent. The presence of magnesium, potassium, calcium, titanium, and iron is detected, but the quantities are lower than 4 wt%.

The element sodium is incorporated into the MFA material by 4.35 wt% higher compared to fly ash due to the hydrothermal treatment with 2 M of NaOH solution [9].

Instrumental neutron activation analysis (INAA) is a method used to determine the qualitative and quantitative analyses of macroelements, microelements, and rare elements in a material.

The advantages of this analysis are that:

1. Through this analysis, more than 30 elements in a sample can be analyzed, even if the elements are found in low levels;
2. It does not require a large quantity of the sample.

The determination of the trace elements of the MFA material was performed by the INAA method and the results are presented in Table 3. This type of analysis is performed in order to establish the trace elements from the adsorbent, especially the content of U, Cs, Ba, Eu, Cd, and Cr [9].

The synthesized material contains higher amounts of Mn (4.46×10^2 ppm), Ba (2.25×10^3 ppm), and Sr (1.39×10^3 ppm).

The crystallographic information concerning the MFA was determined by XRD analyses. The X-ray diffraction pattern is presented in Figure 2. The identification of peaks within the 2θ angle range of 5° to 70° was performed based on data related to peak positions and intensities presented in the literature by Treacy and Higgins (2007) [37].

As can be seen from Figure 2, the most intense phase was identified as quartz (Q). In addition, the XRD analysis confirmed the presence of M (mullite) [38,39]. As was reported in previous studies, the diffraction peaks of quartz and mullite could not be completely dissolved during the treatment [23,36].

Analcime (A) is presented at 2 theta degrees of 33.38° and 42.64°. Clinotobermorite (CT) and chabazite (Cha) are found at 29.72° and 31.1°, respectively. Moreover, the element feldspar (F) is detected at 21° in the synthesized material.

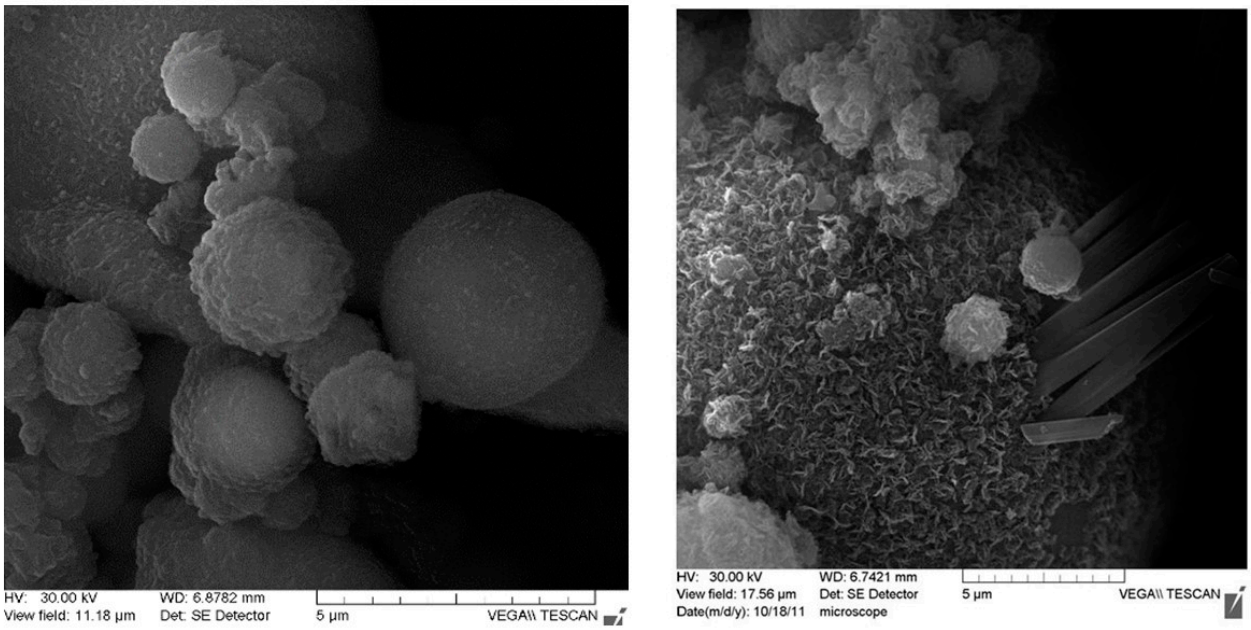

(**a**)

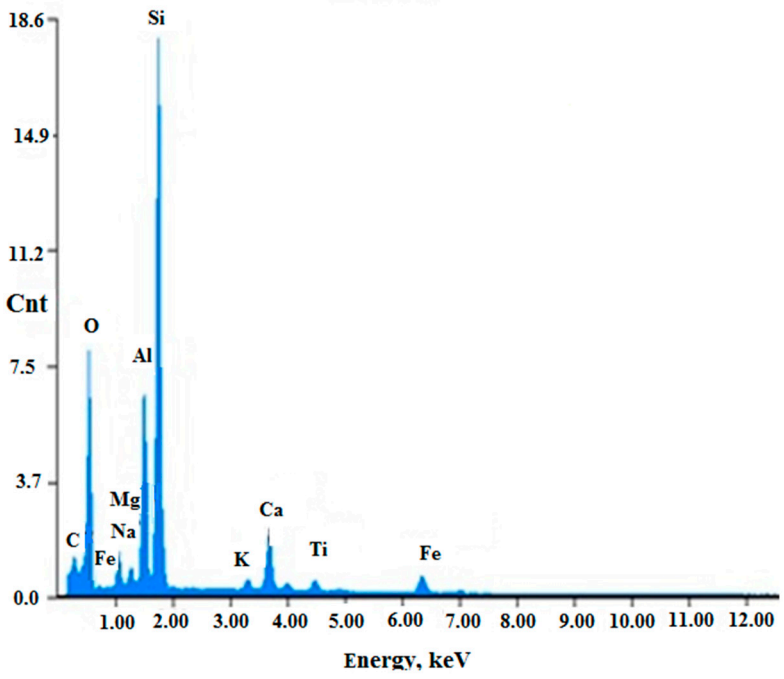

(**b**)

Figure 1. (**a**) SEM analysis of fly ash (FA) (left) and MFA (right); (**b**) EDX analysis of MFA.

Table 2. The chemical composition determined by SEM/EDS (mass%).

Adsorbent	O	Na	Mg	Al	Si	K	Ca	Ti	Fe
FA	43.32	0.79	0.62	19.19	30.81	1.75	1.15	1.54	3.05
MFA	33.85	3.44	0.93	18.33	28.89	0.66	1.44	0.91	4.07

Table 3. The chemical composition of trace elements of the adsorbent as determined by instrumental neutron activation analysis (INAA) (mass in ppm).

Element	A1
Ni	1.13×10^2
Cu	3.09×10^2
As	14.7
Sr	1.39×10^3
Zr	3.41×10^2
V	91.9
Cr	1.36×10^2
Mn	4.46×10^2
Cs	3.77
Ba	2.25×10^3
Ce	1.73×10^2
Eu	2.73
Th	3.02
U	7.39

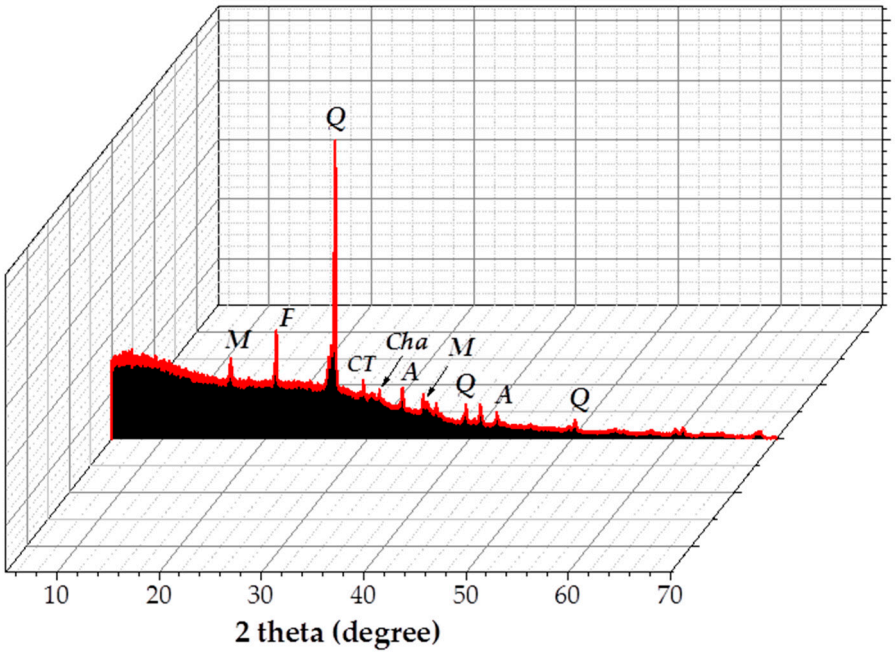

Figure 2. X-ray diffraction pattern.

The analysis concerning the FTIR spectra is presented in Figure 3. The FTIR spectra analysis was used to determine the functional groups present in the synthesized adsorbent. For the analysis, the sample was mixed with KBr and measured within the wavenumber range of 4000–400 cm^{-1}.

The FTIR spectrum possesses similar bands to unmodified fly ash, such as 458 cm^{-1} (O–Si–O or Si–O–Si), 567 cm^{-1} (Al–O–Si and Si–O–Si), 794 cm^{-1} (Si–O), 1040 cm^{-1}, 1653 cm^{-1}, 2364 cm^{-1}, and 3440 cm^{-1} (-OH and H–O–H, respectively).

The BET analysis is shown in Figure 4.

The BET method is used in the study of surfaces in order to determine the areas of porous solids through the physical adsorption of gas molecules. It is used to identify the surface area and the pore sizes of the adsorbent before it is used.

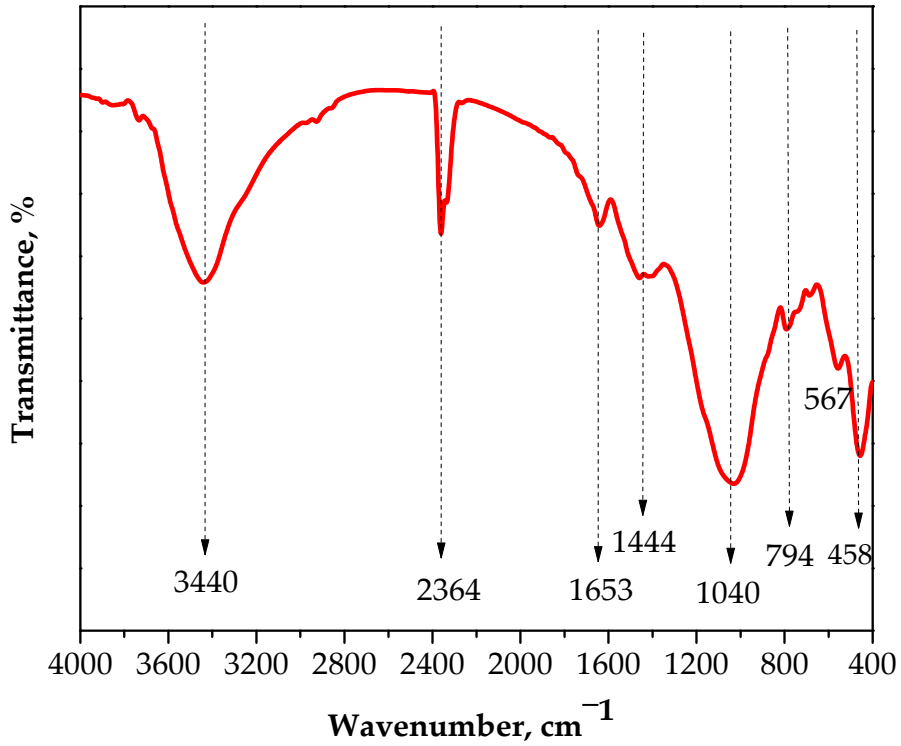

Figure 3. FTIR spectra.

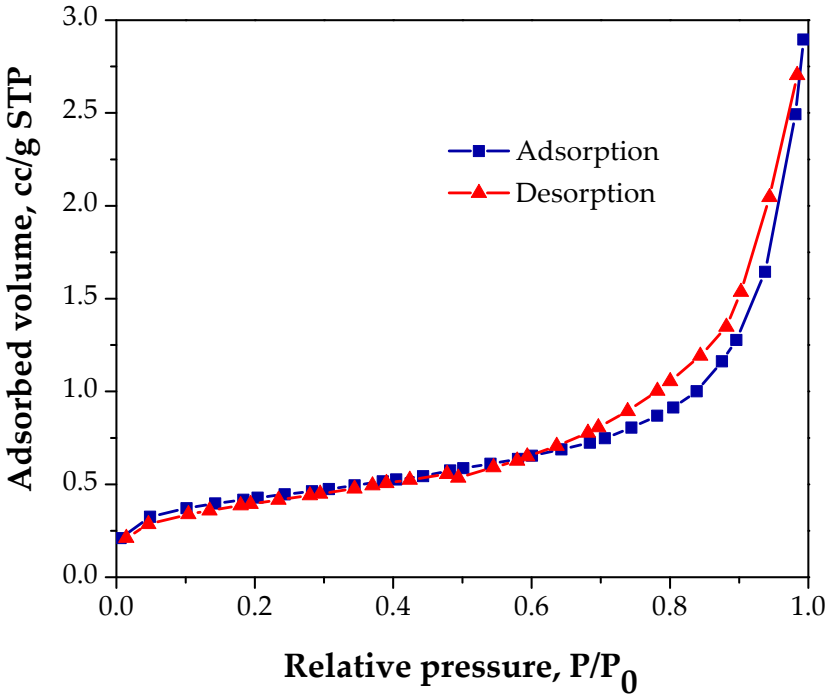

Figure 4. Brunauer–Emmett–Teller (BET) analysis (STP – standard temperature and pressure abbreviation).

The textural properties of MFA were evaluated using the N_2 adsorption–desorption isotherms at 77 K (Figure 4). According to the IUPAC classification, the material presents a type IV isotherm with a small plateau at relatively high pressures, with the H3 type hysteresis loop. Consequently, the results obtained are typical of mesoporous materials.

In terms of the BET analysis, the surface areas of the FA and MFA samples differ. BET investigation reveals that the surface of the MFA adsorbent (calculated from the BET

equation) increased by 1.24 times compared to the fly ash surface. The activation of the fly ash with an alkaline solution for 7 days of contact time leads to an increase in pore volume (0.091 cm^3/g vs. 0.024 cm^3/g for fly ash). The pores of solid materials are classified into three categories: micropores (d < 2 nm), mesopores (2 nm < d < 50 nm), and macropores (d > 50 nm). The average pore volume of 1.594 nm indicates that the prepared material is microporous.

Through thermal analysis, the thermal properties of the synthesized adsorbent are established. Figure 5 presents the thermal analysis data of the MFA adsorbent. In order to determine the mass losses, the analysis was performed in a N_2 atmosphere at temperatures between 20 and 900 °C, with a heating speed of 10 °C/min. The initial mass of the sample was 4.9710 mg.

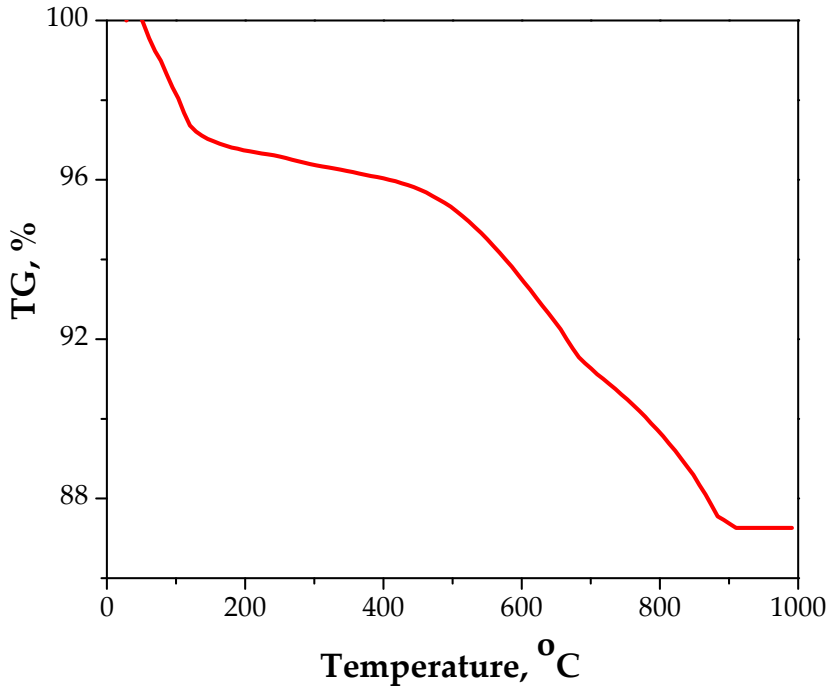

Figure 5. Thermal analysis for the MFA adsorbent.

Analyzing the results presented in Figure 5, it can be seen that the loss on ignition (LOI) and the differential thermal gravimetry (DTG) for the MFA adsorbent takes place in four stages:

1. At 43.90 °C and 82.55 °C, when the loss of moisture occurs (1.81 and 2.22%, respectively);
2. At 500.45 °C, when the loss of crystallization water takes place (2.32%);
3. Between 778.72 and 900 °C, due to the decarbonation of the structure (3.81%).

The thermogravimetric analysis showed that the sample has a total mass loss of 10.16%.

The results obtained in the first stage of the study reveal the capacity of the material as an adsorbent for heavy metals from aqueous solutions, in this case referring to copper ions.

Therefore, after the basic characterization, the synthesized material was employed as an adsorbent for Cu(II) ions from aqueous solution. The batch adsorption experiments were carried out at different pH values. In addition, different amounts of adsorbent and various concentrations of copper ions at different time intervals were measured.

3.2. Effect of Adsorption Parameters

3.2.1. Effect of pH

Firstly, the relationship between the adsorption capacities as a function of pH was investigated. Thus, the effect of the pH on the adsorption of Cu(II) ions on the synthesized adsorbent at three different values—2, 4 and 5—was determined. Note that the adsorption

ability of the adsorbent was not investigated at a pH higher than 5, because the Cu(II) could precipitate. The test was conducted at room temperature with an initial Cu(II) concentration of 500 mg/L, a 10 g/L MFA dose, a contact time of 24 h, and a stirring speed of 300 rpm.

At pH 2, the synthesized material does not have the ability to remove copper ions; for pH 4 and 5, the results are shown in Figure 6.

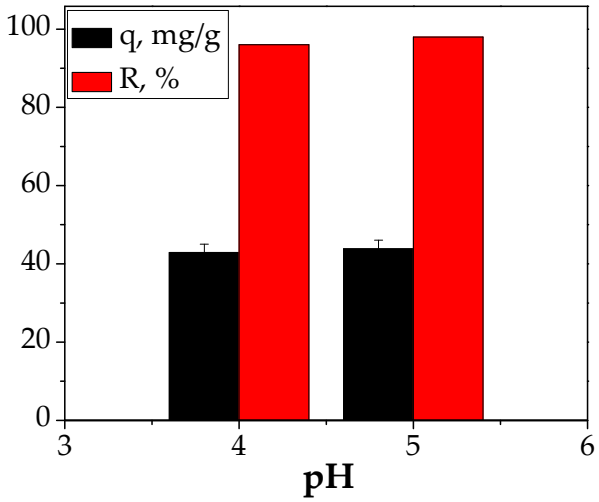

Figure 6. Effect of pH.

As shown in Figure 6, the adsorption process is a function of the pH value. On the other hand, upon increasing the pH value to 4 and 5, adsorption capacities of 42.89 mg/g and 43.85 mg/g were obtained, respectively, corresponding to removal efficiencies of 96 and 98%.

Consequently, it can be stated that the maximum adsorption capacity remains almost constant with an increasing pH value.

3.2.2. Effect of Adsorbent Dose

The influence of this parameter was studied using 1 g/100 mL (10 g/L), 1 g/50 mL (20 g/L), and 1 g/25 mL (40 g/L) MFA/Cu (II) solution ratio, a 300 mg/L initial Cu(II) concentration, and a contact time of 480 min at 300 rpm. The results obtained for the adsorption capacity and removal efficiency are shown in Figure 7.

When the dose is changed, the effect of the MFA dose on the adsorption of Cu(II) ions is visible. From Figure 7, it can be highlighted that the adsorption capacity decreases from 27.6 to 6.18 mg/g with an increase in adsorbent dosage. On the other hand, the removal efficiency decreases from 96 to 93.32%. The results show that the adsorbent dose recommended for the maximum Cu(II) removal efficiency from an initial concentration of 300 mg/L is 1 g adsorbent/100 mL solution. This observation was found in a series of studies [40,41].

3.2.3. Effect of Initial Concentration and Contact Time

Variations in the Cu(II) adsorption capacity and removal efficiency are shown in Figure 8, as a function of the initial Cu(II) concentration and contact time. The experiments were carried out by varying the initial Cu(II) concentration from 300 to 700 mg/L, while the other parameters were kept constant: pH = 5, MFA dose = 10 g/L, 300 rpm, time of contact = 480 min.

From Figure 8, it can be noted that the Cu(II) adsorption process onto MFA is fast in the first few minutes for all three initial concentrations due to the large number of active sites that were available.

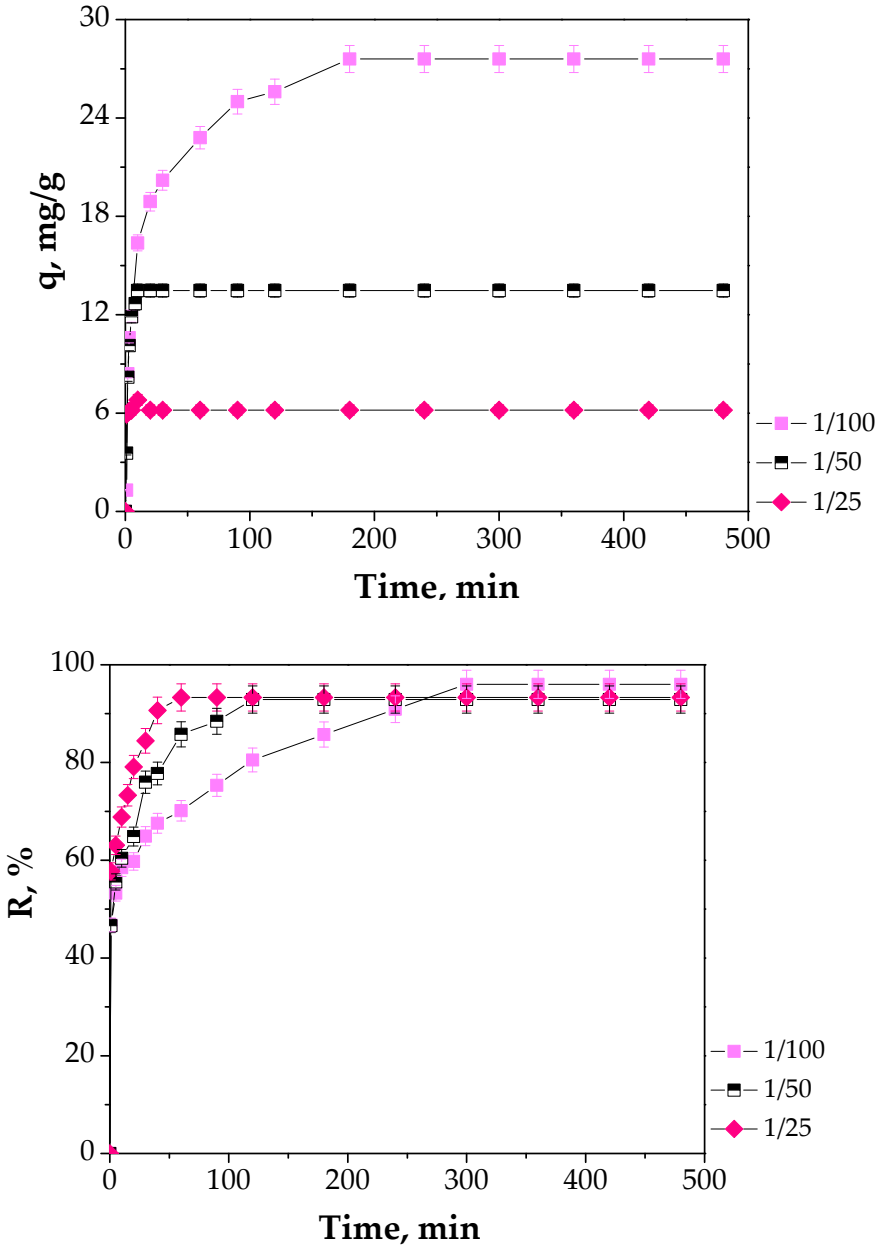

Figure 7. Effect of adsorbent dose.

The adsorption capacity and removal efficiency are dependent on the initial Cu(II) concentration. It should be pointed out that good adsorption capacities and removal efficiencies are obtained in all three cases. Upon increasing the initial Cu(II) concentration from 300 to 700 mg/L, an uptrend in the Cu(II) adsorption capacity was observed from 27.6 to 56.61 mg/g, however, the removal efficiency decreases from 98 to 86.04%. A rational explanation would be that an increase in the driving force took place due to a concentration gradient between the Cu(II) solution and the surface of the MFA adsorbent. The results obtained followed the same trend as the results from the other studies on the adsorption of Cu(II) onto materials based on fly ash [35,42].

The effect of the contact time was also investigated with the MFA adsorbent. As shown in Figure 8, the adsorption capacity and removal efficiency increased as the contact time increased. This fact could be explained by the large surface area of the adsorbent. The maximum adsorption capacity is obtained after approximately 250 min for all concentrations, but with different adsorption capacities and removal efficiencies.

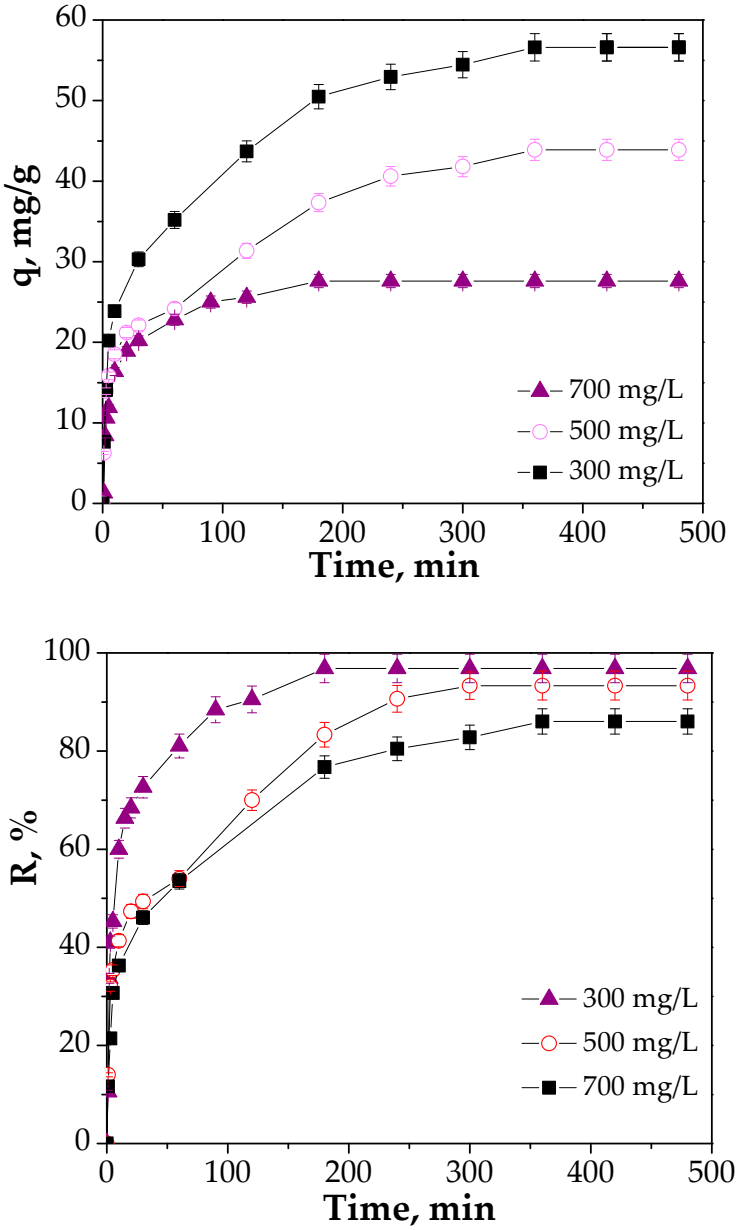

Figure 8. Effect of initial concentration and contact time.

Therefore, a contact time of 250 min is enough for the adsorption to reach equilibrium.

On the basis of the obtained results, it can be concluded that the pH, adsorbent dose, initial Cu(II) concentration, and contact time are factors that affect the adsorption process of Cu(II) by the MFA adsorbent.

3.3. Adsorption Kinetic Study

A kinetic model is a mathematical representation of the rate at which a physical or chemical process takes place [43]. The kinetic study indicates the adsorption rate and the efficiency of the adsorbent. In addition, through the obtained data, the mechanism that takes place can be established.

In the present study, the data obtained were applied to three kinetic models: a pseudo-first order kinetic model (PFO), a pseudo-second order kinetic model (PSO), and an intra-particle diffusion model. This was done in order to evaluate the experimental data obtained at initial Cu(II) concentrations of 300, 500, and 700 mg/L.

The PFO model assumes that the adsorption takes place only at some specific sites. The adsorption kinetics described by the PSO model suppose that the rate limiting step is a chemisorption process. The intraparticle diffusion model [44] assumes that:

1. The transport of adsorbate from the bulk solution to the outer surface of the adsorbent is by molecular diffusion;
2. Internal diffusion, the transport of adsorbate from the particle's surface into an interior site, takes place;
3. The adsorption of the solute particles from the active sites into the interior surface of the pores occurs.

To calculate the kinetic parameters, the equations presented in Table 4 were used [45]:

Table 4. Kinetic models.

Model	Equation
Pseudo-first order kinetic model (PFO)	$log(q_e - q_t) = log\, q_e - \frac{(k_1 t)}{2.303}$
Pseudo-second order kinetic model (PSO)	$\frac{t}{q_t} = \frac{1}{k_2 {q_e}^2} + \frac{t}{q_e}$
Intraparticle diffusion	$q_t = k_i t^{0.5}$+c

where q_t (mg/g) is the amount of Cu(II) ions adsorbed at time t, q_e (mg/g) is the amount of Cu(II) ions adsorbed at equilibrium, k_1 is the pseudo-first order rate constant (1/min), k_2 is the pseudo-second order rate constant (g/mg min), and k_i is the intraparticle diffusion rate constant.

The plots of the data were created for the three initial Cu(II) concentrations of 300, 500, and 700 mg/L (Figure 9). The kinetic parameters are shown in Table 5.

Analyzing Table 5, it can be seen that the experimental data could not be predicted by the PFO model.

On the other hand, the data confirm that the intraparticle diffusion model does not fit the experimental data. The R^2 value for the intraparticle diffusion model was lower compared to the PSO model. In addition, another indicator that supports this statement is that the plots did not pass through the origin.

The high correlation coefficient value, R^2, of 0.9999, and the agreement between $q_{e\ cal}$ and q_{exp} validate the fact that Cu(II) adsorption processes followed the PSO model, which indicated the chemisorption mechanism.

It must be noted that it is difficult to compare the adsorption capacities of some adsorbents in different working adsorption conditions due to factors such as the pH, copper initial concentration, adsorbent doses, and type of synthesis (one of the most important parameters). Taking into account this plausible observation, at the end of the research, a comparison with other materials presented in the literature was shown in order to establish the efficiency of the adsorbent (Table 6).

The data presented in Table 6 show that the MFA adsorbent has a good adsorption capacity, and this fact could imply that the adsorbent can be used for the treatment of wastewater-containing Cu(II) ions.

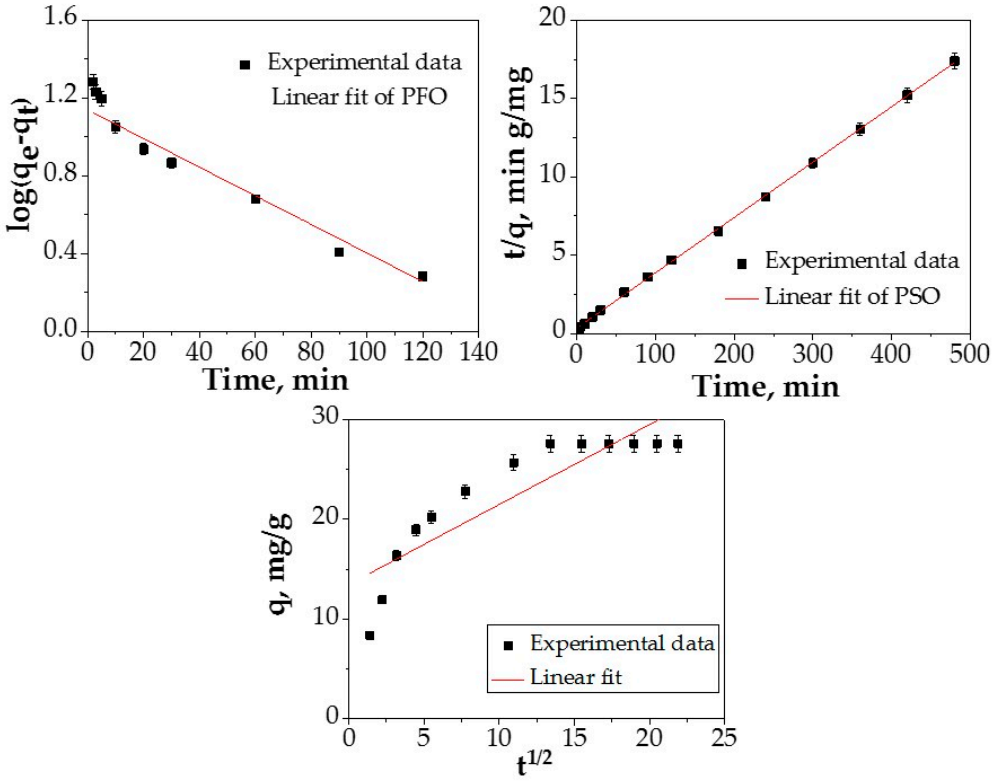

(**a**)

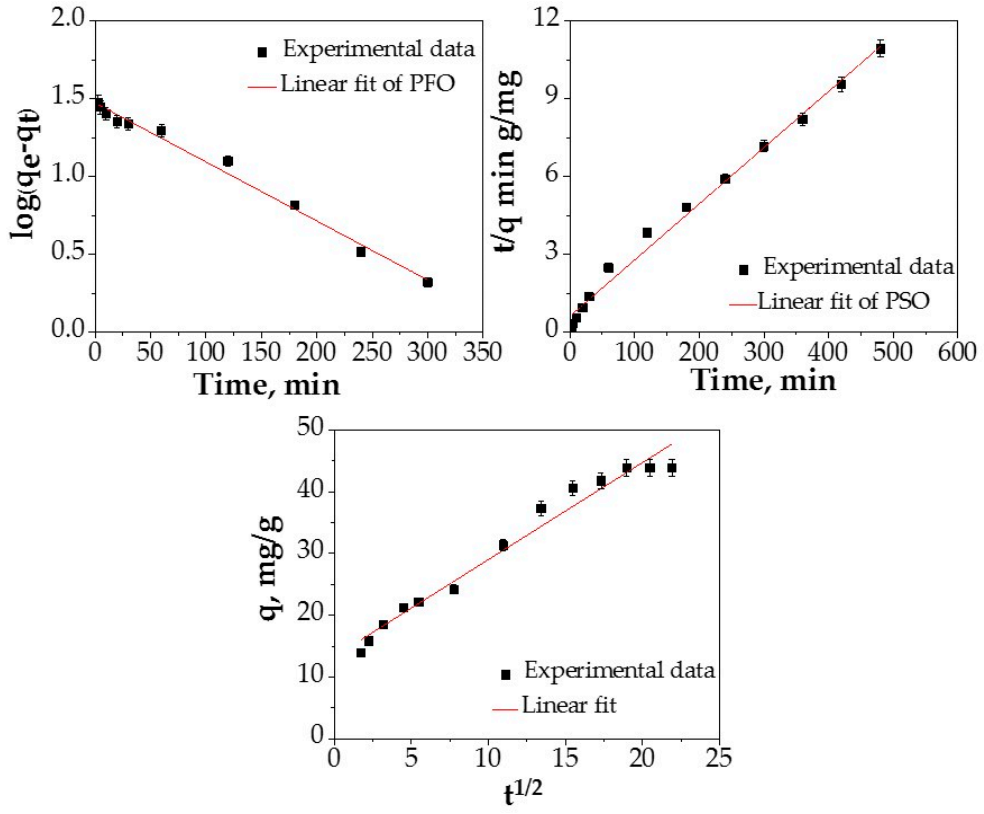

(**b**)

Figure 9. *Cont.*

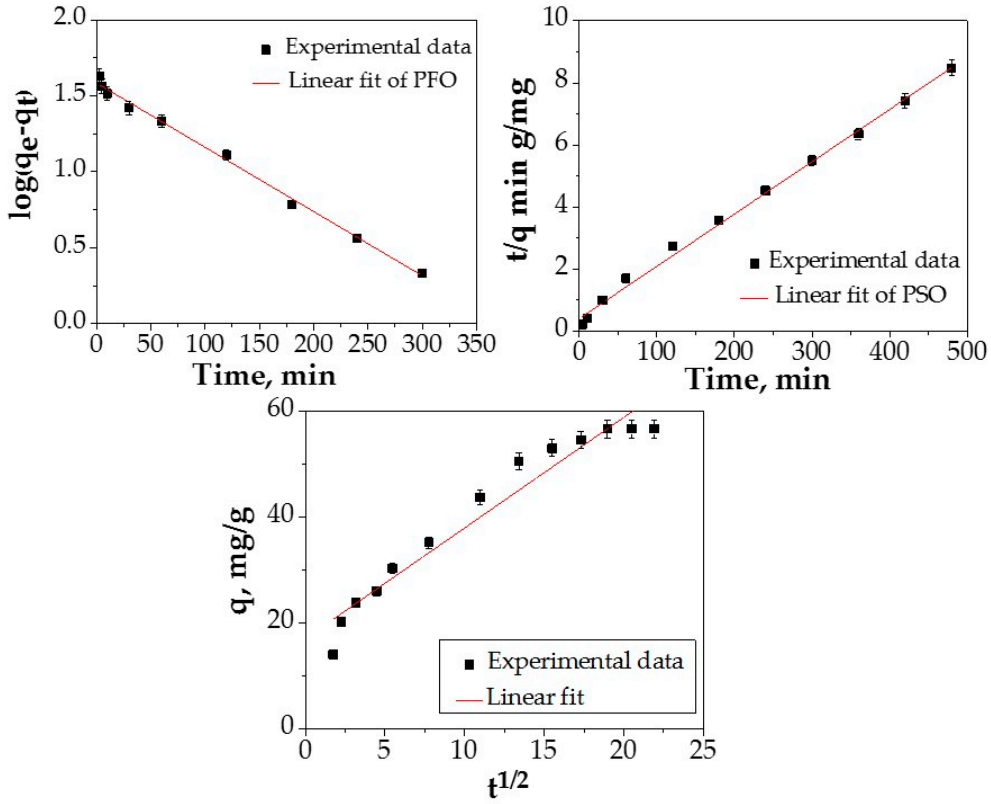

(**c**)

Figure 9. PFO model, PSO model, and intraparticle diffusion model for the adsorption of Cu(II) ions: (**a**) 300 mg/L; (**b**) 500 mg/L; (**c**) 700 mg/L.

Table 5. Kinetic parameters of Cu(II) adsorption onto MFA.

Kinetic Model	Parameters	Values		
		300 mg/L	500 mg/L	700 mg/L
Pseudo-first order	k_1, 1/min	0.0209	0.0092	0.0101
	R^2	0.9169	0.9776	0.9844
Pseudo-second order	$q_{e\,cal}$, mg/g	27.32	45.25	58.48
	k_2, g/mg min	0.0036	0.0010	0.0009
	R^2	0.9994	0.9909	0.9964
Intraparticle diffusion	k_i	1.0899	1.6816	2.1269
	C	9.2665	11.579	15.211
	R^2	0.7392	0.9518	0.9286

Table 6. Comparison of the adsorption capacities for different adsorbents for Cu(II) adsorption.

Adsorbent	q, mg/g	References
FA	14.464	[36]
FA/NaOH (2 M, 70 °C)	6.976–27.904	[36]
FA/NaOH (2 M, 90 °C)	7.056–27.904	[36]
FA/NaOH (5 M, 70 °C)	6.896–27.776	[36]
FA/NaOH (5 M, 90 °C)	6.896–27.904	[36]
Banana peel	1.439–71.429	[46]
FA/NaOH (5 M, 70 °C, US)	23.8	[23]
FA/H_2SO_4	28.09	[40]
CSCMQ copolymer	28.75	[47]
KOH-hydrochar	18.6	[48]
Carbon nanofibers	8.8	[49]
Coal fly ash	8.54	[50]
FA/NaOH (600 °C, 68 h)	39.68	[51]
MFA	27.32–58.48	This study

4. Conclusions

This paper for the first time reports the easy synthesis of one material using fly ash and its application for the removal of copper from aqueous solutions.

The material characterization was performed by SEM, EDX, INAA, XRD, FTIR, BET, and thermal analysis. The material has been successfully synthesized by treating the fly ash with 2 M NaOH for 7 days of contact time.

Furthermore, a series of parameters that influence the adsorption process were evaluated: pH, adsorbent dose, initial concentration, and contact time.

The adsorption of copper ions onto MFA is validated by the pseudo-second order kinetics model.

The new material based on fly ash obtained during this research was found to be efficient for the Cu(II) ion removal in comparison with the adsorbents reported in the literature.

The encouraging results obtained emphasize that the synthesized material is very effective as an adsorbent for copper ions from aqueous solution; extending these studies using real wastewater will permit us to implement this absorbent as an effective, low-cost material in wastewater treatment.

An important advantage that must be stated is that the production of this type of material does not require much energy consumption compared with traditional synthesis.

Author Contributions: Conceptualization, M.H., N.L.; methodology, H.C., L.F.; formal analysis, G.B., G.C., D.B.; investigation, G.B., G.C., R.D.B.; writing—original draft preparation, M.H., G.B., H.C.; writing—review and editing, M.H.; visualization, N.L., D.B.; supervision, M.H. All authors have read and agreed to the published version of the manuscript.

Funding: This research was funded by the UEFISCDI Agency trough Project PN-III-P1-1.2-PCCDI-2017-0152 (Contract No. 75PCCDI/2018).

Institutional Review Board Statement: Not applicable.

Informed Consent Statement: Not applicable.

Data Availability Statement: The data presented in this study are available on request from the corresponding author.

Conflicts of Interest: The authors declare no conflict of interest.

References

1. He, Y.; Zhang, L.; An, X.; Han, C.; Luo, Y. Microwave assistant rapid synthesis MCM-41-NH_2 from fly ash and Cr(VI) removal performance. *Environ. Sci. Pollut. Res.* **2019**, *26*, 31463–31477. [CrossRef] [PubMed]
2. Harja, M.; Cimpeanu, S.M.; Dirja, M.; Bucur, D. Synthesis of zeolites from fly ash and their use as soil amendment. In *Zeolites—Useful Minerals*; Intech Open: London, UK, 2016.
3. Franus, W.; Wdowin, M.; Franus, M. Synthesis and characterization of zeolites prepared from industrial fly ash. *Environ. Monit. Assess.* **2014**, *186*, 5721–5729. [CrossRef] [PubMed]
4. Favier, L.; Harja, M. *TiO2/Fly ash nanocomposite for photodegradation of persistent organic pollutant, In Handbook of Nanomaterials and Nanocomposites for Energy and Environmental Applications*; Kharissova, O., Martínez, L., Kharisov, B., Eds.; Springer: Cham, Switzerland, 2020. [CrossRef]
5. Brostow, W.; Chetuya, N.; Gencel, O.; Hong, H.J.; Menard, N.; Sayana, S. Durability of portland concrete containing polymeric fillers and fly ash. *Mater. Sci.* **2020**, *26*, 103–108. [CrossRef]
6. Sutcu, M.; Erdogmus, E.; Gencel, O.; Gholampour, A.; Atan, E.; Ozbakkaloglu, T. Recycling of bottom ash and fly ash wastes in eco-friendly clay brick production. *J. Clean. Prod.* **2019**, *233*, 753–764. [CrossRef]
7. You, S.; Ho, S.W.; Li, T.; Maneerung, T.; Wang, C.H. Techno-economic analysis of geopolymer production from the coal fly ash with high iron oxide and calcium oxide contents. *J. Hazard. Mater.* **2019**, *361*, 237–244. [CrossRef]
8. Buema, G.; Noli, F.; Misaelides, P.; Sutiman, D.M.; Cretescu, I.; Harja, M. Uranium removal from aqueous solutions by raw and modified thermal power plant ash. *J. Radioanal. Nucl. Chem.* **2014**, *299*, 381–386. [CrossRef]
9. Noli, F.; Buema, G.; Misaelides, P.; Harja, M. New materials synthesized from ash under moderate conditions for removal of toxic and radioactive metals. *J. Radioanal. Nucl. Chem.* **2015**, *303*, 2303–2311. [CrossRef]
10. Samiullah, M.; Aslam, Z.; Rana, A.G.; Abbas, A.; Ahmad, W. Alkali-activated boiler fly ash for Ni (II) removal: Characterization and parametric study. *Water Air Soil Pollut.* **2018**, *229*, 113. [CrossRef]

11. Silliková, V.; Dulanská, S.; Horník, M.; Jakubčinová, J.; Ľubomír, M. Impregnated fly ash sorbent for Cesium-137 removal from water samples. *J. Radioanal. Nucl. Chem.* **2020**, *324*, 1225–1236. [CrossRef]
12. Aydin, T. Development of lightweight ceramic construction materials based on fly ash. *J. Aust. Ceram. Soc.* **2017**, *53*, 109–115. [CrossRef]
13. Kotova, O.B.; Ignatiev, G.V.; Shushkov, D.A.; Harja, M.; Broekmans, M.A. Preparation and properties of ceramic materials from coal fly ash. In *Minerals: Structure, Properties, Methods of Investigation*; Springer: Cham, Switzerland, 2020; pp. 101–107.
14. Asl, S.M.H.; Javadian, H.; Khavarpour, M.; Belviso, C.; Taghavi, M.; Maghsudi, M. Porous adsorbents derived from coal fly ash as cost-effective and environmentally-friendly sources of aluminosilicate for sequestration of aqueous and gaseous pollutants: A review. *J. Clean. Prod.* **2019**, *208*, 1131–1147.
15. Remenárová, L.; Pipíška, M.; Florková, E.; Horník, M.; Rozložník, M.; Augustín, J. Zeolites from coal fly ash as efficient sorbents for cadmium ions. *Clean Techn. Environ. Policy* **2014**, *16*, 1551–1564. [CrossRef]
16. Nguyen, T.C.; Loganathan, P.; Nguyen, T.V.; Jaya Kandasamy, J.; Naidu, R.; Vigneswaran, S. Adsorptive removal of five heavy metals from water using blast furnace slag and fly ash. *Environ. Sci. Pollut. Res.* **2018**, *25*, 20430–20438. [CrossRef] [PubMed]
17. Taylor, A.A.; Tsuji, J.S.; Garry, M.R.; McArdle, M.E.; Goodfellow, W.L.; Adams, W.J.; Menzie, C.A. Critical review of exposure and effects: Implications for setting regulatory health criteria for ingested copper. *Environ. Manag.* **2020**, *65*, 131–159. [CrossRef] [PubMed]
18. Borhade, A.V.; Kshirsagar, T.A.; Dholi, A.G. Eco-Friendly Synthesis of Aluminosilicate Bromo Sodalite from Waste Coal Fly Ash for the Removal of Copper and Methylene Blue Dye. *Arab. J. Sci. Eng.* **2017**, *42*, 4479–4491. [CrossRef]
19. Milićević, S.; Vlahović, M.; Kragović, M.; Martinović, S.; Milošević, V.; Jovanović, I.; Stojmenović, M. Removal of Copper from Mining Wastewater Using Natural Raw Material—Comparative Study between the Synthetic and Natural Wastewater Samples. *Minerals* **2020**, *10*, 753. [CrossRef]
20. Engwa, G.A.; Ferdinand, P.U.; Nwalo, F.N.; Unachukwu, M.N. Mechanism and health effects of heavy metal toxicity in humans. In *Poisoning in the Modern World-New Tricks for an Old Dog?* Intech Open: London, UK, 2019.
21. Ojha, K.; Pradhan, N.C.; Samanta, A.N. Zeolite from fly ash: Synthesis and characterization. *Bull. Mater. Sci.* **2004**, *27*, 555–564. [CrossRef]
22. Curteanu, S.; Buema, G.; Piuleac, C.G.; Sutiman, D.M.; Harja, M. Neuro-evolutionary optimization methodology applied to the synthesis process of ash based adsorbents. *J. Ind. Eng. Chem.* **2014**, *20*, 597–604. [CrossRef]
23. Harja, M.; Buema, G.; Sutiman, D.M.; Cretescu, I. Removal of heavy metal ions from aqueous solutions using low-cost sorbents obtained from ash. *Chem. Pap.* **2013**, *67*, 497–508. [CrossRef]
24. Arbabi, M.; Golshani, N. Removal of copper ions Cu (II) from industrial wastewater: A review of removal methods. *Int. J. Epidemiol.* **2016**, *3*, 283–293.
25. Rachmawati, S.D.; Tizaoui, C.; Hilal, N. Manganese Coated Sand for Copper (II) Removal from Water in Batch Mode. *Water* **2013**, *5*, 1487–1501. [CrossRef]
26. Kang, C.D.; Sim, S.J.; Cho, Y.S.; Kim, W.S. Process development for the removal of copper from wastewater using ferric/limestone treatment. *Korean J. Chem. Eng.* **2003**, *20*, 482–486. [CrossRef]
27. Ulatowska, J.; Stala, Ł.; Nowakowska, A.; Polowczyk, I. Use of synthetic zeolite materials from fly ash to remove copper(II) ions from aqueous solutions. *Physicochem. Probl. Miner. Process.* **2020**, *56*, 114–124. [CrossRef]
28. Querol, X.; Moreno, N.; Umaña, J.C.; Alastuey, A.; Hernandez, E.; Lopez-Soler, A.; Plana, F. Synthesis of zeolites from coal fly ash: An overview. *Int. J. Coal Geol.* **2002**, *50*, 413–423. [CrossRef]
29. Wang, Y.; Guo, Y.; Yang, Z.; Cai, H.; Xavier, Q. Synthesis of zeolites using fly ash and their application in removing heavy metals from waters. *Sci. China Ser. D-Earth Sci.* **2003**, *46*, 967–976. [CrossRef]
30. Hui, K.S.; Chao, C.Y.H.; Kot, S.C. Removal of mixed heavy metal ions in wastewater by zeolite 4A and residual products from recycled coal fly ash. *J. Hazard. Mater.* **2005**, *B127*, 89–101. [CrossRef] [PubMed]
31. Derkowski, A.; Franus, W.; Beran, E.; Czimerova, A. Properties and potential applications of zeolitic materials produced from fly ash using simple method of synthesis. *Powder Technol.* **2006**, *166*, 47–54. [CrossRef]
32. Apiratikul, R.; Pavasant, P. Sorption of Cu^{2+}, Cd^{2+}, and Pb^{2+} using modified zeolite from coal fly ash. *Chem. Eng. J.* **2008**, *144*, 245–258. [CrossRef]
33. Hsu, T.C.; Yu, C.C.; Yeh, C.M. Adsorption of Cu^{2+} from water using raw and modified coal fly ashes. *Fuel* **2008**, *87*, 1355–1359. [CrossRef]
34. Boycheva, S.V.; Zgureva, D.M. Surface studies of fly ash zeolites via adsorption/desorption isotherms. *Bulg. Chem. Commun.* **2016**, *48*, 101–107.
35. Qiu, Q.; Jiang, X.; Lv, G.; Chen, Z.; Lu, S.; Ni, M.; Yan, J.; Lin, X.; Song, H.H.; Cao, J. Adsorption of copper ions by fly ash modified through microwave-assisted hydrothermal process. *J. Mater. Cycles. Waste Manag.* **2019**, *21*, 469–477. [CrossRef]
36. Harja, M.; Buema, G.; Sutiman, D.M.; Munteanu, C.; Bucur, D. Low cost adsorbents obtained from ash for copper removal. *Korean J. Chem. Eng.* **2012**, *29*, 1735–1744. [CrossRef]
37. Treacy, M.M.; Higgins, J.B. *Collection of Simulated XRD Powder Patterns for Zeolites*, 5th ed.; Elsevier: Amsterdam, The Netherlands, 2007.
38. Forminte, L.; Ciobanu, G.; Buema, G.; Lupu, N.; Chiriac, H.; de Castro, C.G.; Harja, M. New materials synthesized by sulfuric acid attack over power plant fly ash. *Rev. Chim.* **2020**, *71*, 48–58. [CrossRef]

39. Cretescu, I.; Harja, M.; Teodosiu, C.; Isopescu, D.N.; Chok, M.F.; Sluser, B.M.; Salleh, M.A.M. Synthesis and characterisation of a binder cement replacement based on alkali activation of fly ash waste. *Process Saf. Environ. Protect.* **2018**, *119*, 23–35. [CrossRef]
40. Buema, G.; Lupu, N.; Chiriac, H.; Roman, T.; Porcescu, M.; Ciobanu, G.; Burghila, D.V.; Harja, M. Eco-Friendly Materials Obtained by Fly Ash Sulphuric Activation for Cadmium Ions Removal. *Materials* **2020**, *13*, 3584. [CrossRef]
41. Buema, G.; Lupu, N.; Chiriac, H.; Ciobanu, G.; Kotova, O.; Harja, M. Modeling of solid-fluid non-catalytic processes for nickel ion removal. *Rev. Chim.* **2020**, *71*, 4–15. [CrossRef]
42. Yang, Y.; Zhang, P.; Jiang, J.; Dai, Y.; Wu, M.; Pan, Y.; Ni, L. Synthesis and properties of magnetic zeolite with good magnetic stability from fly ash. *J. Sol-Gel Sci. Technol.* **2018**, *87*, 408–418. [CrossRef]
43. Yusuff, A.S.; Popoola, L.T.; Babatunde, E.O. Adsorption of cadmium ion from aqueous solutions by copper-based metal organic framework: Equilibrium modeling and kinetic studies. *Appl. Water Sci.* **2009**, *9*, 106. [CrossRef]
44. Yalcin, M.; Gurses, A. The Adsorption Kinetics of Cethyltrimethylammonium Bromide (CTAB) onto Powdered Active Carbon. *Adsoprtion* **2004**, *10*, 339–348.
45. Marcos, C.; Medoro, V.; Adawy, A. Modified Vermiculite as Adsorbent of Hexavalent Chromium in Aqueous Solution. *Minerals* **2020**, *10*, 749. [CrossRef]
46. Hossain, M.A.; Ngo, H.H.; Guo, W.S.; Nguyen, T.V. Removal of Copper from Water by Adsorption onto Banana Peel as Bioadsorbent. *Int. J. Geomate.* **2012**, *2*, 227–234. [CrossRef]
47. Shah, P.U.; Raval, P.N.; Shah, N.K. Adsorption of Copper from an Aqueous Solution by Chemically Modified Cassava Starch. *J. Mater. Environ. Sci.* **2015**, *6*, 2573–2582.
48. Koottatep, T.; Fakkaew, K.; Tajai, N.; Polprasert, C. Isotherm models and kinetics of copper adsorption by using hydrochar produced from hydrothermal carbonization of faecal sludge. *J. Water Sanit. Hyg. Dev.* **2017**, *7*, 102–110. [CrossRef]
49. García-Díaz, I.; López, F.A.; Alguacil, F.J. Carbon Nanofibers: A New Adsorbent for Copper Removal from Wastewater. *Metals* **2018**, *8*, 914. [CrossRef]
50. Darmayanti, L.; Notodarmodjo, S.; Damanhuri, E. Removal of copper (II) ions in aqueous solutions by sorption onto fly ash. *J. Eng. Technol. Sci.* **2017**, *49*, 546–559. [CrossRef]
51. Joseph, I.V.; Tosheva, L.; Doyle, A.M. Simultaneous removal of Cd (II), Co (II), Cu (II), Pb (II), and Zn (II) ions from aqueous solutions via adsorption on fau-type zeolites prepared from coal fly ash. *J. Environ. Chem. Eng.* **2020**, *8*, 103895. [CrossRef]